Density of states and light-vibration coupling coefficient in B_2O_3 glasses with different thermal history

N. V. Surovtsev,[1] A. P. Shebanin,[2] and M. A. Ramos[3]
[1]*Institute of Automation and Electrometry, Russian Academy of Sciences, Pr. Ak.Koptyuga, 1, Novosibirsk, 630090, Russia*
[2]*United Institute of Geology, Geophysics, and Mineralogy, Russian Academy of Sciences, Novosibirsk, 630090 Russia*
[3]*Departamento de Física de la Materia Condensada, C-III, Instituto "Nicolás Cabrera," Universidad Autónoma de Madrid, Cantoblanco, E-28049 Madrid, Spain*

(Received 11 May 2002; revised manuscript received 15 October 2002; published 17 January 2003)

The terahertz density of vibrational states (i.e., the *boson peak*) for several B_2O_3 glasses with different thermal histories was evaluated from specific heat data. It was found that the boson peak density of states is lower for more annealed glasses, the position of the boson peak maximum ν_{BP} shifting to higher frequencies. Low-frequency Raman spectra have been recorded for the same set of glasses. By comparison of Raman and low-temperature specific heat data the light-vibration coupling coefficient has been extracted. The coupling coefficient $C(\nu)$ can be described by a linear dependence $C(\nu)=A(\nu/\nu_{BP}+0.5)$ in the spectral range $0.5\nu_{BP}-2\nu_{BP}$ for the whole set of B_2O_3 glasses, the amplitude A being independent of annealing.

DOI: 10.1103/PhysRevB.67.024203 PACS number(s): 63.50.+x, 64.70.Pf, 63.20.Pw

I. INTRODUCTION

The vibrational motion of glasses with frequencies ν in the terahertz range (0.1–3 THz) continues to be a very interesting and widely studied topic. The lack of long-range order in the glass structure leads somehow to an excess in the vibrational density of states over the Debye behavior, a maximum in $g(\nu)/\nu^2$ that has become known as the ''boson peak.'' THz vibrations of glasses are studied by several experimental techniques: low-temperature specific heat and thermal conductivity,[1] inelastic neutron scattering,[2,3] x-ray scattering,[4–6] infrared absorption,[7] etc. In addition, useful information has become available from molecular dynamics simulations.[8,9] Low-frequency Raman scattering is a very often used experimental technique,[10] which relates the density of vibrational states, $g(\nu)$ (the number of vibrational modes per unit frequency and per unit volume), with the light-scattering spectrum via the so-called light-vibration coupling coefficient $C(\nu)$,[11]

$$I(\nu)=C(\nu)g(\nu)\frac{n+1}{\nu}, \tag{1}$$

where $I(\nu)$ is the Raman intensity for the Stokes side of the spectrum and n is the Bose factor.

In spite of numerous experimental and theoretical studies, the nature of THz vibrational excitations cannot be considered as well understood. There are different views about the boson peak origin. The key question remains to identify the wave function of boson peak vibrations. Since the light-vibration coupling coefficient is a convolution of the correlator of the vibrational wave function,[11] the study of $C(\nu)$ seems very appealing to check different models and approaches. An especially interesting issue in this respect would be to study the coupling coefficient of glasses of the same chemical compound, but with a different THz vibrational spectrum. This goal can be achieved by using the fact that many properties of a glass depend on its thermal history.

The physical properties of B_2O_3 glasses change remarkably on applying different annealing treatments.[12] The mass density of glassy B_2O_3 is a good parameter to characterize the physical properties of differently annealed samples.[13,14] Low-temperature specific heat measurements reveal changes of the THz density of vibrational states for differently annealed B_2O_3 glasses[15]—the broad peak in a C_P/T^3 plot decreases when the sample density increases. For the same set of B_2O_3 glasses it was found that the boson peak position in Raman spectra[16] shifts to higher frequencies for more annealed samples, whereas the high-frequency modes do not show discernible changes. The goal of the present study is to find out for this set of B_2O_3 glasses with different thermal histories (i) the density of vibrational states and (ii) the Raman-scattering coupling coefficient. The vibrational density of states will be obtained from the low-temperature specific heat data by solving the corresponding integral equation (a numerical technique for this procedure was proposed recently in Refs. 17 and 18). In order to analyze quantitatively the changes in the magnitude of the coupling coefficient $C(\nu)$, we have performed a normalization of the boson peak spectrum by high-frequency modes and have improved the precision of the Raman experiment in comparison with earlier measurements.[16]

In the next section, we will describe the samples used, the experimental techniques for Raman-scattering measurements, and the procedure employed to obtain the vibrational density of states from specific heat data. In Sec. III, the experimental results will be presented. Then, these results will be critically discussed in Sec. IV, under different views and models currently found in the literature. Section V will summarize our main conclusions.

II. EXPERIMENT

Six boron-oxide glass samples (labeled D1–D5, W2; cf. Table I) studied earlier in Refs. 13–16 have been used in the present work. The samples were annealed over different periods of time at temperatures in the vicinity of T_g, and then

TABLE I. Basic parameters of the different B_2O_3 glasses: ρ, density (Ref. 13); v_D, Debye sound velocity (Ref. 16); C_{Debye}, cubic coefficient of the specific heat within Debye's theory; ν_{BP}, boson-peak maximum position from $g(\nu)/\nu^2$.

Sample	Thermal treatment	ρ[g/cm^3]	v_D [km/s]	C_{Debye} [μJ/gK^4]	ν_{BP} [cm^{-1}]
D1	As quenched	1.804	2.055	7.82	15
D2	585 K, 48 h	1.806	2.068	7.66	15.5
D3	530 K, 50 h	1.826	2.104	7.19	16.5
D4	525 K, 92 h	1.823	2.124	7.01	16.5
D5	480 K, 170 h	1.834	2.158	6.64	17.5
W2	490 K, 100 h	1.866	2.233	5.89	19

the density was measured at room temperature. The basic characteristics of the samples (parameters of thermal treatment, as well as measured densities and sound velocities) are presented in Table I. The preparation procedure of the B_2O_3 samples is described in detail in Ref. 13. Samples D1–D5 have a very low water content (less than 0.5 mol %, see Table I). Sample W2 has an OH^- content of 5.8 mol % as determined by infrared spectroscopy.[14] The five "dry" glasses exhibit a very similar $T_g \approx 570$ K. For most physical properties and especially for acoustic ones, the mass density of B_2O_3 samples is the main parameter that characterizes the physical properties of B_2O_3 glasses.

Raman right-angle experiments were performed using an argon laser with a wavelength of 514.5 nm, a power of 150 mW, and a double-grating monochromator U-1000. All experiments were conducted at room temperature. HH-polarization geometry was used in the depolarized scattering experiment (H denotes horizontal orientation of the electrical field of the electromagnetic wave relative to the scattering plane). This polarization scattering scheme allows us to reduce the effect of depolarization of light on sample surfaces for recorded spectra, as discussed in Ref. 16. Spectral slits of 4 cm^{-1} were used. Three scans over spectral ranges 10–210 cm^{-1}, 770–850 cm^{-1}, and 1100–1700 cm^{-1} were recorded for every sample. The spectrum for the frequency range 770–850 cm^{-1} was measured in order to control the quality of the depolarization scattering conditions, since the strong mode near 808 cm^{-1} is highly polarized and its intensity in the depolarized experiment enables us to estimate the leakage of polarized component. For one sample (W2) the polarized scattering was then also measured in order to find the experimental depolarization coefficient for the mode at 808 cm^{-1}. The depolarization coefficient was found to be about 0.04—that is, close to magnitudes previously reported for this mode[19,20]—and demonstrates a negligible leakage of the polarized component for HH geometry. Figure 1 presents the Raman scattering spectra of a B_2O_3 sample (D1) for the low-frequency (10–210 cm^{-1}) and high-frequency (1100–1700 cm^{-1}) spectral ranges. In a previous work,[16] it was shown that the high-frequency modes do not show discernible changes and, therefore, can be used for normalization of the low-frequency spectrum. Low-frequency spectra were normalized by the integral over the high-frequency modes (1100–1700 cm^{-1}) after subtraction of the background, which is shown in Fig. 1 as a dashed line.

On the other hand, the density of vibrational states was evaluated from the low-temperature specific heat $C_P(T)$ (data from Ref. 15) by solving the integral equation[21]

$$C_V(T) = \frac{k_B}{\rho}\int_0^\infty g(\nu)\left(\frac{h\nu}{k_B T}\right)^2 \frac{\exp(h\nu/k_B T)}{[\exp(h\nu/k_B T)-1]^2} d\nu. \qquad (2)$$

Here ρ is the mass density and k_B is Boltzmann's constant (the difference between C_V and C_P was neglected). The procedure for solving this equation was described in Refs. 17 and 18. The so-extracted density of states is reliable in the frequency range up to 40–50 cm^{-1} (this high-frequency limit is related to the limiting range of specific heat data[17]).

The light vibration-coupling coefficient is given by

$$C(\nu) \propto \frac{\rho I_{\mathrm{nor}}(\nu)\nu}{g(\nu)[n(\nu,T)+1]}, \qquad (3)$$

where $I_{\mathrm{nor}}(\nu)$ is the low-frequency Raman spectrum normalized by high-frequency modes. Equation (3) follows from Eq. (1) by taking into account that low-frequency spectra are normalized by high-frequency modes (so that the number of modes per unit volume which are responsible for the high-frequency spectrum is proportional to the density). In the evaluation of $C(\nu)$, the weak quasiharmonic shift of the density of states between room temperature and about 10 K due to the sound-velocity variation $[v(10\ \mathrm{K})/v(300\ \mathrm{K}) \approx 1.027)$ (Ref. 16) was considered.

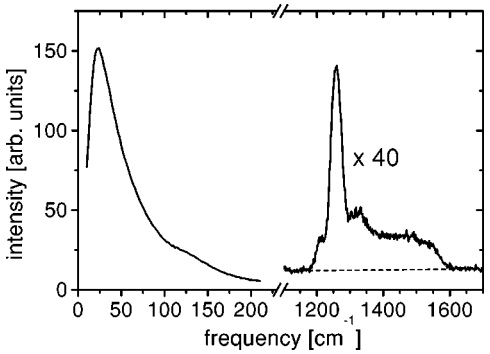

FIG. 1. Raman spectrum of the D1 sample. The dashed line shows the background, which is subtracted before the normalization procedure.

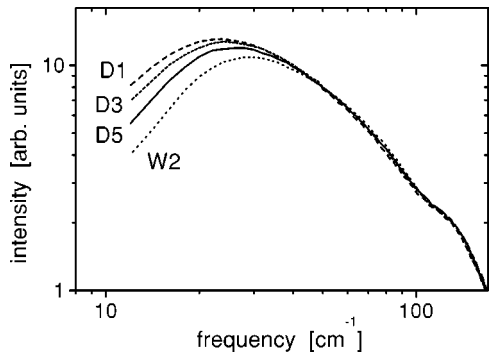

FIG. 2. Low-frequency Raman spectra of different B_2O_3 samples.

III. RESULTS

Figure 2 shows the low-frequency Raman-scattering spectra of three dry samples (D1, D3, and D5) corresponding to two extreme and one intermediate cases of annealing. The spectra have been normalized by the high-frequency Raman modes as described above. In Fig. 2 the logarithmic scale is used for clarity. In this figure, it can be seen that the main difference among spectra is related to variations of the lower-frequency part–the light-scattering intensity decreases for better annealed samples. The high-frequency side of the boson peak looks the same for all samples. The Raman spectrum of wet sample W2 is also included in Fig. 2 for comparison. However, the W2 spectral intensity was multiplied by a factor of 0.88 in order to match the right side of the spectra. The reason for such a correction is the following. In the wet sample 5.8% of oxygen atoms are in hydroxyl groups instead of being normal bridging oxygens. Since the change of one bridging oxygen in the B_2O_3 structure by an OH^- group leads to the appearance of two distorted BO_3 groups, the number of high-frequency modes will be changed roughly by a factor of $(1-2\times0.058)\approx0.88$ for the W2 sample. This estimate coincides well with that found experimentally. Therefore one can conclude that both annealing and increasing the water content produce the same effect on the Raman spectra: to decrease the low-frequency side of the boson peak with increasing density, without altering the high-frequency side (see Fig. 2).

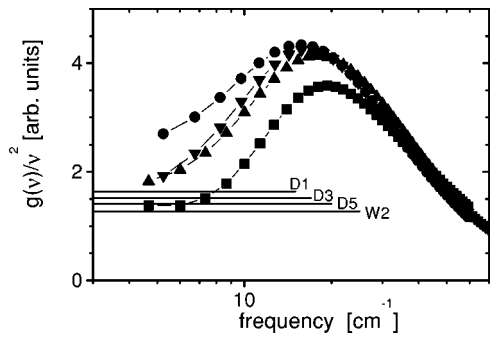

FIG. 3. Density of vibrational states $g(\nu)/\nu^2$ for samples D1 (circles), D3 (down triangles), D5 (up triangles), and W2 (squares). Lines indicate the calculated Debe density of states.

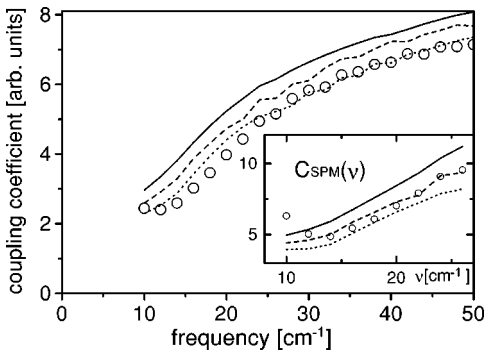

FIG. 4. Light-vibration coupling coefficient $C(\nu)$ of B_2O_3 glasses: D1 (solid line), D3 (dashed line), D5 (dotted line), and W2 (circles). The inset shows $C_{SPM}(\nu)$ calculated by means of Eq. (4) for the same samples.

Figure 3 presents the density of vibrational states as $g(\nu)/\nu^2$, evaluated from specific heat data[15] following the procedure described above. This plot shows that the magnitude of the maximum (boson peak) decreases and its frequency position increases for more annealed (more dense) samples. The spectral positions of the maxima are shown in Table I. It is to be stressed that these boson-peak frequencies ν_{BP} are always different and lower than those directly obtained from reduced Raman-intensity spectra, such as ν_0 in Table I of Ref. 16, the reason being that the former correspond to maxima in $g(\nu)/\nu^2$ and the latter do not, since $C(\nu)$ is not constant but rather a monotonically increasing function of ν. Similarly to the behavior observed for the Raman spectra, the evolution of the $g(\nu)/\nu^2$ boson peak reflects mainly a decrease in the density of states at low energies with increasing density. A similar result has been found recently for the vibrational density of states in normal and densified SiO_2 glasses.[22]

Vibrational densities of states for the studied set of B_2O_3 glasses were evaluated within Debye's theory from measured mass densities and sound velocities. Average Debye velocities were calculated from Brillouin scattering data[13,16] as described in Ref. 16, taking into account the temperature variation. The cubic coefficient of the Debye term in the specific heat is also shown in Table I for each glass and the corresponding Debye density of states indicated in Fig. 3 by lines. It can be observed that the magnitude of the $g(\nu)/\nu^2$ maximum decreases for more annealed or dense glasses concurrently with the Debye level.

The calculated light-vibration coupling coefficients is shown in Fig. 4 for several representative B_2O_3 samples, which exhibit the typical increase with increasing frequency. It is also seen that the coupling coefficient is not the same for B_2O_3 samples with different thermal history—for a given frequency the coupling coefficient magnitude decreases for more annealed glasses.

IV. DISCUSSION

It is well known that THz acoustic excitations (boson peak) of glassy materials cannot be simply described by well-defined plane waves (Debye approximation) in contrast

with crystalline solids.[1,23] Computer simulations have also given evidence for the normal modes of vibrations of a glassy structure not being pure plane waves.[24–26] The remaining question is what are those THz vibrations and how can they be described. At present, there is no generally accepted solution to this problem. There exist different phenomenological models aiming at a description of acousticlike vibrations in glasses. One may distinguish two basic kinds of approaches: several authors assume the coexistence at low enough frequencies of Debye-like acoustic phonons with *excess* vibrational excitations responsible for the boson-peak, whereas others consider that disorder in glasses makes that distinction unsuitable in the whole frequency range of the boson-peak feature. Since most of these models are quite flexible, it is not easy to choose among them from the experimental data. Therefore, we will limit ourselves to briefly discuss our experimental findings in the light of the most usual approaches found in the literature for the boson-peak problem.

The decrease of the vibrational density of states in the lower-energy region for more annealed samples (see Fig. 3) could be understood in the spirit of the soft-potential model (SPM),[27,28] such as was done in Ref. 22, where a similar decrease in the low-energy side of the boson peak for densified SiO_2 glass was explained by a decrease in the number of the low-energy soft potentials, likely related to a decrease of the void space.[22] However, this interpretation does not provide a clear explanation of the coupling coefficient behavior (see Fig. 4). In the framework of the SPM,[29] non-Debye behavior of vibrations results from the coexistence of quasilocalized vibrations (*soft modes*) and Debye-like acoustic phonons, and hence one should calculate the coupling coefficient solely for the soft-mode density of states $C_{SPM}(\nu)$ devoid of the Debye contribution:

$$C_{SPM}(\nu)=\frac{\nu I(\nu)}{(n+1)[g(\nu)-g_{Deb}(\nu)]}, \tag{4}$$

$g_{Deb}(\nu)$ being the Debye density of states.

In the standard SPM, the polarizability tensor is simply assumed to be independent of the specific shape of the single-well potential and hence $C_{SPM}(\nu)=\text{const}$.[29,30] This assumption has been questioned in Ref. 31, where it was argued that different parameters of the soft potentials should correspond to different shapes of the molecular groups involved in the soft mode and hence to different polarizability coefficients, as well as in Ref. 32, where it was suggested that phononlike vibrational states would also contribute to Raman spectra. The inset of Fig. 4 shows the soft-mode coupling coefficient $C_{SPM}(\nu)$ determined by Eq. (4). One can observe that $C_{SPM}(\nu)$ depends on the thermal history of the glass even more strongly than $C(\nu)$. It is also remarkable that $C_{SPM}(\nu)$ is frequency dependent in contrast with the standard SPM assumption.[29,30] Therefore, our results seem to confirm that the drastic separation between Debye-like acoustic modes—noncontributing to Raman scattering—and soft modes—with $C_{SPM}(\nu)=\text{const}$—and hence the use of Eq. (4), is not justified at boson-peak frequencies.

An approach reminiscent of the SPM was presented by Engberg *et al.*,[3] who postulated the coexistence of random-phase and in-phase modes at frequencies around the boson peak. The in-phase modes are identified with sound waves, though their density of states (DOS) is not assumed to follow necessarily the Debye law. Within this model[3] only random-phase modes contribute to low-frequency Raman scattering. Unfortunately, there is no direct procedure to extract the random-phase contribution and test the model without conducting complementary neutron-scattering experiments in our glasses. If we accept, however, this approach, our experimental results (see Fig. 4) would imply that the share of the random-phase contribution decreases for more annealed or densified glass samples. In addition, one may conclude that the relative spectral distributions of random- and in-phase modes either do not change with thermal treatment or change in parallel, since average coupling coefficients exhibit a similar frequency dependence.

From hyper-Raman scattering experiments in vitreous SiO_2, Hehlen *et al.*[33] found that the boson-peak spectrum looks very different for Raman and hyper-Raman cases. This experimental result was interpreted by the existence of two kind of motions: acousticlike ones, which can be active in Raman scattering, and local or nonacoustic motions (i.e., rotation or rocking of regular SiO_4 tetrahedra), which only contribute to hyper-Raman scattering, since they do not modulate the polarizability. On the other hand, this particular situation does not apply to B_2O_3, where the rocking of BO_3 units *does* modulate the polarizability and it is thus active in Raman scattering.[23] In this case, the authors of Ref. 23 seem to follow the same above-mentioned view of Engberg *et al.*,[3] assuming that only random-phase (here not forbidden) modes are Raman active with $C(\nu)=\text{const}$, the apparent frequency dependence of the coupling coefficient being due to the nonvisibility of part of the total DOS (the in-phase modes). In our opinion, this kind of approach does not allow one to understand the universal character of the quasilinear dependence of the coupling coefficient near the boson-peak maximum for different types of glasses.[34] Here we would like to note that the conclusions obtained in Ref. 33 are not an unambiguous consequence of their experiment. Indeed, the difference between Raman and hyper-Raman experiments can be explained in the framework of the vibrational wave function suggested in Ref. 35, where the boson-peak wave function shares properties of both localized and extended excitations: at short distances, displacements of atoms are coherent and the wave function correlator is similar to a vibration localized in the cluster; for the correlator at longer distances, however, the vibrations have a diffusive (extended) character (see the Appendix).

Let us finally consider the approach that around the boson peak there is only one, predominantly acousticlike, type of vibrations, so that they cannot be separated into independent kinds of vibrations at a given frequency. The coupling coefficient therefore retains its proper physical meaning. In Ref. 38, it was shown that the coupling coefficient for SiO_2 glasses exhibits a frequency dependence

$$C(\nu)\propto\nu+\text{const} \tag{5}$$

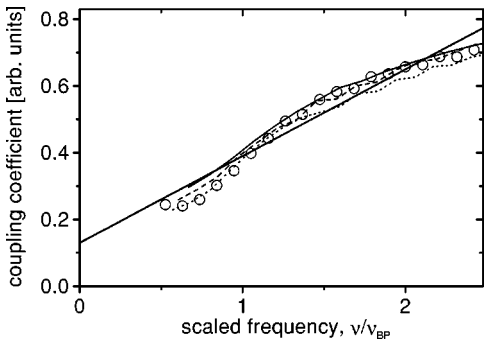

FIG. 5. Scaling plot of the light-vibration coefficient $C(\nu)$ of B_2O_3 glasses (the same symbols as in Fig. 4). The thick solid line is a fit to $(\nu/\nu_{BP}+0.5)$.

near the boson-peak maximum. This expression has been recently tested[34] for a large set of different glasses. It was found that the coupling coefficient for all those glasses presents a linear frequency dependence near the boson-peak maximum in the range $0.5\nu_{BP}-2\nu_{BP}$ [where ν_{BP} is the boson-peak maximum position for $g(\nu)/\nu^2$]. The observed universality of $C(\nu)$ was considered as supporting the idea that boson-peak vibrations cannot be separated into different kinds of vibrations, but rather related to the complex character of the vibration wave function. In that work,[34] it was also found that about half of glasses analyzed had a simple linear proportionality for the coupling coefficient $[C(\nu)\propto\nu]$ and the other half of them could be scaled to a single master plot with a general dependence

$$C(\nu)\propto A(\nu/\nu_{BP}+0.5). \tag{6}$$

In particular, it was found that the coupling coefficient of B_2O_3 glass followed the dependence given by Eq. (6). In Fig. 5 the coupling coefficient of our set of B_2O_3 glasses is plotted versus frequency scaled by its corresponding boson-peak position. As can be seen from this figure, the scaled coupling coefficients fall into the same master plot. A small oscillation of the coupling coefficients around the linear dependence is an artifact of the solution of Eq. (2) due to the limited precision or range of the specific heat data.[17] Equation (6) seems therefore to describe well the behavior of the coupling coefficients in Fig. 5. Furthermore, $C(\nu)$ of B_2O_3 glasses with different thermal history can be well represented by Eq. (6) with the same constant A for all glasses, whereas ν_{BP} varies appreciably (see Table I). The magnitudes of $C(\nu)$ are the same if the coupling coefficient is considered versus the scaled frequency (in contrast to Fig. 4). Since $C(\nu)$ reflects the correlator of the vibrational wave function, this result underlines the interrelation between the boson-peak position and the wave function, and stresses the utility of parameter ν_{BP} for describing terahertz dynamics in glasses.

V. CONCLUSION

We have presented in this work a study of THz vibrational motion (boson peak) in a set of B_2O_3 glasses with different thermal histories and water content. The vibrational density of states was determined by solving the integral equation for the low-temperature specific heat. It was found that the magnitude of the lower-energy side of the boson peak is clearly decreased and the position of the boson-peak maximum ν_{BP} gradually increased for more annealed or densified samples. By comparing the low-frequency Raman scattering and the vibrational density of states, the light-vibration coupling coefficient $C(\nu)$ was obtained. These results were discussed within different models or approaches found in the current literature. In particular, it was found that the coupling coefficients for the whole set of B_2O_3 glasses can be well described as $C(\nu)=A^*(\nu/\nu_{BP}+0.5)$ with the same constant A, whereas ν_{BP} changes appreciably.

ACKNOWLEDGMENTS

Useful discussions about the boson-peak problem with E. Duval, V. K. Malinovsky, V. N. Novikov, E. Rössler, A. P. Sokolov, and J. Wiedersich are appreciated. This work was supported by the Interdisciplinary Science Fund at the Russian Foundation for Basic Research of the Siberian Division of the Russian Academy of Sciences (project No. 7) and by RFFI Grant No. 02-02-16112. M.A.R. acknowledges financial support from Spanish MCyT under Project No. BFM2000-0035-C02.

APPENDIX

Here we would like to show that the boson-peak wave function suggested in Ref. 35 allows us to explain the difference between Raman and hyper-Raman spectra, even if only one type of vibrational excitation exists at a given frequency. In this case, the effective coupling coefficient of hyper-Raman scattering, $C_{HRS}(\nu)$, has to be frequency independent, whereas $C(\nu)$ presents a linear frequency dependence for the Raman-scattering spectrum.

For acoustic-type excitations the coupling coefficients of Raman and hyper-Raman experiments read similarly:

$$C(\nu)\propto\int \partial\vec{r}\langle P(0)P^*(\vec{r})\rangle\langle s^{\nu}(0)s^{\nu *}(\vec{r})\rangle, \tag{A1}$$

$$C_{HRS}(\nu)\propto\int \partial\vec{r}\langle P_{HRS}(0)P^*_{HRS}(\vec{r})\rangle\langle s^{\nu}(0)s^{\nu *}(\vec{r})\rangle. \tag{A2}$$

Here $s^{\nu}(\vec{r})$ is the strain of an acoustic vibration with frequency ν, $\langle\cdots\rangle$ means configurational and statistical averaging, $P(\vec{r})$ is the elastooptic constant, $P_{HRS}(\vec{r})$ is the elasto-hyperpolarizability constant, an analog of the elasto-optic constant for the hyperpolarizability β, and $P_{HRS}(\vec{r})=\partial\beta/\partial s$. In Eqs. (A1) and (A2), the exponential factor $\exp(i\vec{q}\vec{r})$, where $\vec{q}$ is the scattering wave vector of the experiments been neglected, since the phonon mean free path is much shorter than the light wavelength. In these equations

we omit the polarization indexes for simplicity, since we are not interested in the polarization properties of the light-scattering experiments.

The differences between hyper-Raman and Raman coupling coefficients can be related to different properties of the correlators for P and P_{HRS}. It is naturally assumed that in glasses the fluctuation of the linear polarizability is much weaker than that of the hyperpolarizability. Indeed, the nonlinear susceptibility is expected to vary strongly in disordered media, being higher in local defective places. Therefore, whereas for Raman scattering one can neglect the fluctuating part of the elastooptic constants, the fluctuating part of the elasto-hyperpolarizability constant can dominate the hyper-Raman spectrum. This assumption for hyper-Raman scattering is supported by the conclusion from Hehlen *et al.*[33]—they argued that the full depolarization of the experimental hyper-Raman spectrum rules out the case that the average *non-fluctuating* part of the hyperpolarizability could dominate the spectrum. The above-mentioned difference between Raman and hyper-Raman scattering leads to different frequency dependences for the coupling coefficients.

Thus the integral over the wave function correlator is only relevant for the Raman coupling coefficient

$$C(\nu) \propto \int \partial \vec{r} \langle s^{\nu}(0) s^{\nu *}(\vec{r}) \rangle. \tag{A3}$$

According to the model of Ref. 35 this integral is separated into two parts: the first one is for short distances, where the wave function of the vibration mimics the localized feature; the second one is for longer distances, where the wave function has a diffusive character:

$$C(\nu) \propto \int_0^{|\vec{r}|=R} \partial \vec{r} \langle s^{\nu}(0) s^{\nu *}(\vec{r}) \rangle + \int_{|\vec{r}|=R}^{\infty} \partial \vec{r} \langle s^{\nu}(0) s^{\nu *}(\vec{r}) \rangle, \tag{A4}$$

where R is a typical radius of the nanoscale inhomogeneity in glass structure. The wave function in the first term behaves as a localized vibration and this is precisely the case described in the Shuker-Gammon model.[11] Then, the first term should be frequency independent. The diffusive character of the boson-peak vibrations determines the frequency behavior of the second term in Eq. (A4). In Ref. 36, it was shown that the diffusive nature of acoustic vibrations leads to $C(\nu) \propto \nu$, and hence the second term in Eq. (A4) is proportional to frequency. Thus, the localized-extended character of the boson peak vibrations leads to the linear frequency dependence of the Raman coupling coefficient.[35]

If the correlator of the fluctuating part of the elastohyperpolarizability constant has a correlation length shorter than the distance at which the diffusive character of the boson-peak vibration becomes important, then the coupling coefficient (A2) is dominated by the local-like character of the vibrational mode. This is the case described in the Shuker-Gammon model.[11] Therefore, $C_{HRS}(\nu)$ is frequency independent, in agreement with experiment.[33] Thus, under resonable assumptions both Raman- and hyper-Raman-scattering spectra can be described by only one (acoustic) type of vibrations. This consideration is partially supported by Ref. 37, where the thermal conductivity of glassy SiO_2 is described by acoustic vibrations. In that work, it was concluded that the excess density of states contributing to the observed heat transport in the plateau temperature range would have an acousticlike character.

[1] *Amorphous Solids: Low-Temperature Properties*, edited by W.A. Phillips (Springer, Berlin, 1981).

[2] U. Buchenau, N. Nücker, and A.J. Dianoux, Phys. Rev. Lett. **53**, 2316 (1984); U. Buchenau, M. Prager, N. Nücker, A.J. Dianoux, N. Ahmad, and W.A. Phillips, Phys. Rev. B **34**, 5665 (1986).

[3] D. Engberg, A. Wischnewski, U. Buchenau, L. Börjesson, A.J. Dianoux, A.P. Sokolov, and L.M. Torell, Phys. Rev. B **58**, 9087 (1998); **59**, 4053 (1999).

[4] P. Benassi, M. Krisch, C. Masciovecchio, V. Mazzacurati, G. Monaco, G. Ruocco, F. Sette, and R. Verbeni, Phys. Rev. Lett. **77**, 3835 (1996).

[5] M. Foret, E. Courtens, R. Vacher, and J.B. Suck, Phys. Rev. Lett. **77**, 3831 (1996).

[6] A. Matic, D. Engberg, C. Masciovecchio, and L. Börjesson, Phys. Rev. Lett. **86**, 3803 (2001).

[7] U. Strom and P.C. Taylor, Phys. Rev. B **16**, 5512 (1977).

[8] S.N. Taraskin and S.R. Elliott, Europhys. Lett. **36**, 37 (1997).

[9] J. Horbach, W. Kob, and K. Binder, Eur. Phys. J. B **19**, 531 (2001).

[10] J. Jäckle, in *Amorphous Solids: Low-Temperature Properties*, edited by W.A. Phillips (Springer, Berlin, 1981).

[11] R. Shuker and R.W. Gammon, Phys. Rev. Lett. **25**, 222 (1970).

[12] F.C. Everstein, J.M. Stevels, and H.I. Waterman, Phys. Chem. Glasses **1**, 123 (1960).

[13] M.A. Ramos, J.A. Moreno, S. Vieira, C. Prieto, and J.F. Fernández, J. Non-Cryst. Solids **221**, 170 (1997).

[14] M.A. Ramos, S. Vieira, C. Prieto, and J.F. Fernández, in *Borate Glasses, Crystals and Melts*, edited by A.C. Wright, S.A. Feller, and A.C. Hannon (The Society of Glass Technology, Sheffield, 1997), pp. 207–214.

[15] E. Pérez-Enciso, M.A. Ramos, and S. Vieira, Phys. Rev. B **56**, 32 (1997).

[16] N.V. Surovtsev, J. Wiedersich, A.E. Batalov, V.N. Novikov, M.A. Ramos, and E. Rossler, J. Chem. Phys. **113**, 5891 (2000).

[17] N.V. Surovtsev, *Optoelectronics, Instrumentation and Data Processing*, No. 4 (Allerton Press, New York, 2001), p. 43.

[18] N.V. Surovtsev, Phys. Rev. E **64**, 061102 (2001).

[19] A.K. Hassan, L.M. Torell, L. Börjesson, and H. Doweidar, Phys. Rev. B **45**, 12 797 (1992).

[20] M.A. Ramos, S. Vieira, and J.M. Calleja, Solid State Commun. **64**, 455 (1987).

[21] C. Kittel, *Introduction to Solid State Physics* (Wiley, New York, 1986).

[22] Y. Inamura, M. Arai, O. Yamamuro, A. Inaba, N. Kitamura, T.

Otomo, T. Matsuo, S.M. Bennington, and A.C. Hannon, Physica B **263-264**, 299 (1999).
[23] E. Courtens, M. Foret, B. Hehlen, and R. Vacher, Solid State Commun. **117**, 187 (2001).
[24] V. Mazzacurati, G. Ruocco, and M. Sampoli, Europhys. Lett. **34**, 681 (1996).
[25] S.N. Taraskin and S.R. Elliott, Phys. Rev. B **56**, 8605 (1997).
[26] S.N. Taraskin and S.R. Elliott, Phys. Rev. B **61**, 12 017 (2000).
[27] V.G. Karpov, M.I. Klinger, and F.N. Ignat'ev, Sov. Phys. JETP **57**, 439 (1983); M.A. Il'in, V.G. Karpov, and D.A. Parshin, *ibid.* **65**, 165 (1987).
[28] U. Buchenau, Yu.M. Galperin, V.L. Gurevich, and H.R. Schober, Phys. Rev. B **43**, 5039 (1991); U. Buchenau, Yu.M. Galperin, V.L. Gurevich, D.A. Parshin, M.A. Ramos, and H.R. Schober, *ibid.* **46**, 2798 (1992).
[29] For a review, see D.A. Parshin, Phys. Solid State **36**, 991 (1994).
[30] V.L. Gurevich, D.A. Parshin, J. Pelous, and H.R. Schober, Phys. Rev. B **48**, 16 318 (1993).
[31] S.N. Yannopoulos and G.N. Papatheodorou, Phys. Rev. B **62**, 3728 (2000).
[32] L.I. Deich, Phys. Rev. B **51**, 8131 (1995).
[33] B. Hehlen, E. Courtens, R. Vacher, A. Yamanaka, M. Kataoka, and K. Inoue, Phys. Rev. Lett. **84**, 5355 (2000).
[34] N.V. Surovtsev and A.P. Sokolov, Phys. Rev. B **66**, 054205 (2002).
[35] N.V. Surovtsev and A.P. Sokolov, cond-mat/0206295 (unpublished).
[36] V.N. Novikov, in *Proceedings of the XIVth International Conference on Raman Scattering*, edited by N.-T. Yu and X.-Y. Li (Wiley, New York, 1994), p. 766.
[37] R. Vacher, J. Pelous, and E. Courtens, Phys. Rev. B **56**, R481 (1997).
[38] A. Fontana, R. Dell'Anna, M. Montagna, F. Rossi, G. Viliani, G. Ruocco, M. Sampoli, U. Buchenau, and A. Wischnewski, Europhys. Lett. **47**, 56 (1999).